Electrochemical, EPR, and Crystal Structure Studies on Mixed-ligand 4,5-Dimercapto-1,3-dithia-2-thione Phosphine Complexes of Nickel, Palladium and Platinum, M(dmit)(dppe) and Pt(dmit)$(PPh_3)_2$

RAMON VICENTE, JOAN RIBAS

Departament de Quimica Inorganica, Facultat de Quimica, Universitat de Barcelona, Diagonal 647, 08028 Barcelona, Spain

XAVIER SOLANS, MANUEL FONT-ALTABA

Departament de Cristallografia i Mineralogia, Universitat de Barcelona, Gran Via 525, 08007 Barcelona, Spain

ALAIN MARI, PHILIPPE DE LOTH and PATRICK CASSOUX

Laboratoire de Chimie de Coordination du CNRS, Unité 8241 par convention à l'Université Paul Sabatier, 205 Route de Narbonne, 31077 Toulouse Cedex, France

(Received December 24, 1986)

Abstract

Complexes of the type M(dmit)$(Phos)_2$ (M = Ni, Pd, Pt; H_2dmit = 4,5-dimercapto-1,3-dithia-2-thione; $(Phos)_2$ = dppe = 1,2-bis-diphenylphosphinoethane. M = Pt; $(Phos)_2 = (PPh_3)_2$) have been studied by means of X-ray diffraction method, and electrochemical techniques coupled with EPR spectroscopy. The crystal structure of Pt(dmit)(dppe) has been determined: this compound crystallizes in the monoclinic space group $P2_1/n$ with $a = 18.267(3)$, $b = 16.903(3)$, $c = 9.748(2)$ Å, $\beta = 95.50(2)^\circ$ and $Z = 4$. The environment of the platinum atom is nearly square-planar (Pt-P = 2.254(3), Pt–S = 2.311(3) Å) with very slight tetrahedral distortion. The cyclic voltammetry parameters for the oxidation and the reduction of the studied complexes have been determined in CH_2Cl_2: Ni(dmit)(dppe) undergoes a quasi-reversible one-electron reduction step. Pd(dmit)(dppe) undergoes an irreversible two-electron reduction step. Both Pt(dmit)(dppe) and Pt(dmit)$(PPh_3)_2$ do not undergo reduction. All three M(dmit)(dppe) (M = Ni, Pd, Pt) undergo a reversible one-electron oxidation step, the Pt(dmit)$(PPh_3)_2$ a quasi-reversible one. EPR studies of the electrogenerated complexes show that the reduction of Ni(dmit)(dppe) is metal-based and that the $[Ni(dmit)(dppe)]^-$ is a nickel(I) species. The oxidation of the M(dmit)(dppe) complexes is ligand-based and the unpaired electron in the $[M(dmit)dppe]^+$ species is mainly delocalized on the dmit ligand.

Introduction

The $dmit^{2-}$ ligand (H_2dmit = 4,5-dimercapto-1,3-dithia-2-thione) forms transition metal complexes which are the source of conductive [1, 2], and even superconductive [3], materials. Some of these complexes may be used as molecular model systems of metal-tetrathiolato polymers $(MC_2S_4)_n$ [4, 5]. These polymers have aroused great interest because of their high compaction powder conductivity (up to 50 Ω^{-1} cm^{-1} [6, 7]). They have been the subject of several research works including their transport properties and degree of partial oxidation [5, 8], magnetic behavior [5, 9] and formation mechanism [4–7].

The formation mechanism of these polymers that we have proposed [5] was based upon the unexpected obtaining of mononuclear metal complexes, M(dmdto)$(Phos)_2$ and M(dmit)$(Phos)_2$ ($(Phos)_2$ = dppe = 1,2-bis-diphenylphosphinoethane; $(Phos)_2$ = $(PPh_3)_2$; H_2dmdto = 4,5-dimercapto-1,3-dithia-2-one). These complexes were characterized by elemental analysis, IR spectra and mass spectra [4], but none of the crystal structures had been determined. We report here the crystal structure of one member of these series, Pt(dmit)(dppe).

Another pending question regarding the metal-tetrathiolato polymers concerns the origin of their degree of partial oxidation (DPO) which plays an important role in determining their conductivity [5, 8]: does this DPO result from the accessibility of partial oxidation states for the ligand, or does the electron density in the metal orbitals significantly change as the oxidation state changed? In the present work we have studied the redox behavior of the M(dmit)(dppe) (M = Ni, Pd, Pt) and Pt(dmit)$(PPh_3)_2$ model complexes, and the products of several redox reactions have been studied by EPR spectroscopy.

Experimental

Synthesis and Selection of X-ray Data Crystals

The M(dmit)(dppe) (M = Ni(II), Pd(II) and Pt(II)) and Pt(dmit)$(PPh_3)_2$ complexes were prepared as previously reported [4].

0020-1693/87/$3.50

TABLE I. Crystallographic Data and Data Collection Parameters for Pt(dmit)(dppe)

Formula	$C_{29}H_{24}P_2PtS_5$
Molecular weight	789.87
Crystal system	monoclinic
Space group	$P2_1/n$
a (Å)	18.267(3)
b (Å)	16.903(3)
c (Å)	9.748(2)
β (°)	95.50(2)
V (Å^3)	2996(2)
Z	4
D_{calc} (g cm^{-3})	1.75
Crystal colour and shape	red prism
Radiation, λ (Å)	Mo Kα, 0.71069
Diffractometer	Philips Pw-1100
Absorption coefficient (cm^{-1})	48.8
Scan technique	ω-scan
Scan width (°)	1
Scan speed (° s^{-1})	0.03
Data collected	3108
2θ Scan range (°)	4–45
Unique data with $I > 2.56(I)$	3091
R %(F_o)	4.1
R_w %(F_o)	4.7

Single crystals of Pt(dmit)(dppe), suitable for crystal structure determination were obtained by slow evaporation of a solution of this compound in chloroform under a dry N_2 flow, in the dark and at room temperature. This solution is air- and light-stable for a few days only; after a longer period of time, decomposition is evident.

Collection and Reduction of X-ray Diffraction Data

A red prism crystal (0.08 X 0.08 X 0.2 mm) of Pt(dmit)(dppe) was mounted on a Philips Pw-1100 four-circle X-ray diffractometer and the crystal structure elucidated. The unit-cell parameters were obtained from least-squares fit based on the setting angles of 25 reflections ($6° < \theta < 9°$). Intensity data were collected using the ω-scan technique (scan width 1°, scan speed 0.03° s^{-1}; Mo Kα radiation, λ = 0.71069 Å). 3108 independent reflections were recorded in the range $4 < 2\theta < 45°$. The final data set was constitued of 3091 'observed' independent reflections having $I > 2.5\sigma(I)$. Intensity data were corrected for Lorentz polarization, but not for absorption. The details of data collection are summarized in Table I.

Solution and Refinement of the Structure

The structure was solved by direct methods, using the MULTAN system of computer programs [10]. An E-map from the set of phases with the highest combined figure of merit revealed peaks for 28 atoms, and subsequent weighted Fourier map gave the remaining non-hydrogen atoms. The structure was refined isotropically and anisotropically by full-matrix least-squares method, using the SHELX76 computer program [11]. The function minimized was $w||F_o| - |F_o||^2$, where $w = (\sigma^2(F_o) + 0.0051 |F_o|^2)^{-1}$, f, f′ and f″″ were taken from International Table for X-ray Crystallography [12]. The final R factor was 0.041 (R_w = 0.047) for all observed reflections. Several atoms of dppe ligand and S(5) show high temperature coefficients which indicate a disorder in their localization. Table II lists the atomic coordinates of the non-hydrogen atoms with their standard deviations.

TABLE II. Fractional Atomic Coordinates (x10^5 for Pt; x10^4 otherwise) of Non-hydrogen Atoms of Pt(dmit)(dppe) (e.s.d.s in parentheses)

	x/a	y/b	z/c
Pt	68856(2)	8705(2)	16084(4)
P(1)	7221(2)	596(2)	−502(3)
C(1)	7969(7)	−155(8)	−357(13)
C(2)	8038(14)	−500(15)	979(21)
P(2)	7455(2)	−276(2)	2245(3)
C(101)	7586(16)	1441(7)	−1392(11)
C(102)	8141(11)	1868(12)	−732(19)
C(103)	8435(10)	2524(11)	−1390(25)
C(104)	8176(11)	2752(13)	−2643(20)
C(105)	7580(15)	2420(12)	−3198(20)
C(106)	7257(10)	1733(11)	−2612(18)
C(111)	6524(6)	136(6)	−1671(11)
C(112)	5888(6)	−121(8)	−1205(13)
C(113)	5363(7)	−538(9)	−2084(16)
C(114)	5494(9)	−669(9)	−3423(17)
C(115)	6122(11)	−414(10)	−3897(15)
C(116)	6650(9)	−12(10)	−3040(14)
C(201)	8041(7)	−303(8)	3830(15)
C(202)	8069(8)	−945(8)	4697(14)
C(203)	8553(10)	−970(10)	5922(16)
C(204)	8982(12)	−340(14)	6275(26)
C(205)	8921(14)	337(16)	5525(37)
C(206)	8460(11)	312(13)	4186(30)
C(211)	6832(9)	−1097(7)	2243(13)
C(212)	6114(9)	−960(9)	2395(16)
C(213)	5596(10)	−1608(10)	2410(21)
C(214)	5887(16)	−2392(11)	2108(27)
C(215)	6569(17)	−2500(13)	2037(30)
C(216)	7102(11)	−1853(10)	2057(21)
S(1)	6227(2)	1970(2)	786(3)
C(S1)	5939(6)	2342(6)	2274(13)
C(S2)	6104(6)	2010(6)	3543(12)
S(2)	6628(2)	1172(2)	3821(3)
S(3)	5399(2)	3194(2)	2250(4)
S(4)	5754(2)	2497(2)	4919(4)
C(5)	5339(7)	3270(7)	4010(16)
S(5)	4939(3)	4013(3)	4735(7)

Electrochemistry

Voltammetric measurements and controlled potential electrolysis were performed with use of a home-

made microcomputer controlled instrumentation with ohmic resistance compensation [13].

Rigorously deaerated dichloromethane (CH_2Cl_2, Merck), purified by a previously reported method [14], was used as a solvent and $(n\text{-}Bu_4N)ClO_4$ (0.1 M) as supporting electrolyte. Solutions were deaerated by means of a stream of argon bubbling for 15 min and an argon blanket was maintained above the solutions during the electrochemical measurements.

Potentials were referred *versus* an Ag/AgCl (0.1 M KCl) electrode separated from the bulk of the solution by a medium porosity fritted disk. The potential for the one-electron oxidation of ferrocene is 420 mV and 460 mV *versus* the Ag/AgCl (0.1 M KCl) electrode with or without ohmic resistance compensation, respectively. A platinum wire auxiliary electrode was used in conjunction with a platinum disc working electrode (TACUSSEL EDI rotating electrode, area 3.14 mm^2).

Coulometry was performed at 210 K on a large area platinum electrode. Due to the experimental requirements (temperature and atmosphere control) a previously described [15] electrolysis cell allowing combined coulometry–EPR studies was used.

EPR Spectra

The EPR spectra of reduced or oxidized species in CH_2Cl_2 glass were recorded on a Bruker ER 200 TT spectrometer, equipped with a Bruker B-NM20 gaussmeter and a EIP 548 microwave frequency counter, operating at X-band frequencies.

The experimental spectra were simulated and EPR parameters, g and A (^{31}P hyperfine coupling constants) determined by using the program POWDER [16] based on the paper of Weil [17]. The g-strain values and the angles of the g and A tensors have been neglected because of the experimentally observed large linewidth. In the simulation of the spectrum of the $[Ni(dmit)(dppe)]^-$ complex, the percentage of an organic radical impurity has been determined, after digitalization of the experimental spectra and normalization to an arbitrary surface unity, by using the SIMPLEX-subroutine of the program MINUIT [18].

Results and Discussion

Structure of the Pt(dmit)(dppe) Complex

The unit cell contains four Pt(dmit)(dppe) molecules. The molecular structure is shown in Fig. 1, together with the atom-labelling scheme. The bond lengths and angles are listed in Table III. The Pt atom displays a slightly distorted square-planar coordination. The Pt–P mean distance is equal to 2.254(3) Å (to be compared with 2.247 Å in *cis*-$Pt(PMe_3)_2Cl_2$) [19] and the Pt–S mean distance,

TABLE III. Bond Lengths (Å) and Angles (°) of Pt(dmit)(dppe)

Pt–S(1)	2.315(3)	S(1)–Pt–S(2)	90.0(1)
Pt–S(2)	2.308(3)	S(1)–Pt–P(1)	91.5(1)
Pt–P(1)	2.251(3)	P(1)–Pt–P(2)	85.2(1)
Pt–P(2)	2.258(3)	S(2)–Pt–P(2)	93.6(1)
S(1)–C(S1)	1.710(11)	S(1)–Pt–P(2)	174.0(1)
S(2)–C(S2)	1.716(11)	S(2)–Pt–P(1)	175.9(1)
C(S1)–C(S2)	1.366(16)	C(S1)–S(1)–Pt	101.2(4)
C(S1)–S(3)	1.744(11)	C(S2)–S(2)–Pt	101.3(4)
C(S2)–S(4)	1.747(10)	S(1)–C(S1)–C(S2)	123.9(8)
S(3)–C(5)	1.734(15)	S(2)–C(S2)–C(S1)	123.6(8)
S(4)–C(5)	1.714(15)	S(3)–C(S1)–C(S2)	115.3(8)
C(5)–S(5)	1.645(12)	S(4)–C(S2)–C(S1)	115.9(8)
P(1)–C(1)	1.860(10)	S(3)–C(S1)–S(1)	120.8(7)
P(2)–C(2)	1.810(15)	S(4)–C(S2)–S(2)	120.5(7)
C(1)–C(2)	1.425(20)	C(S1)–S(3)–C(5)	97.9(6)
P(1)–C(101)	1.830(10)	C(S2)–S(4)–C(5)	98.0(6)
P(1)–C(111)	1.801(10)	S(3)–C(5)–S(4)	112.8(10)
P(2)–C(201)	1.795(14)	S(3)–C(5)–S(5)	123.7(10)
P(2)–C(211)	1.794(15)	S(4)–C(5)–S(5)	123.5(9)
		C(1)–P(1)–Pt	109.5(4)
		C(101)–P(1)–Pt	114.6(4)
		C(101)–P(1)–C(1)	105.7(6)
		C(111)–P(1)–Pt	115.4(4)
		C(111)–P(1)–C(1)	102.9(6)
		C(111)–P(1)–C(101)	107.7(5)
		C(2)–C(1)–P(1)	113.3(9)
		P(2)–C(2)–C(1)	119.1(0)
		C(2)–P(2)–Pt	107.4(5)
		C(201)–P(2)–Pt	118.7(5)
		C(201)–P(2)–C(2)	102.4(9)
		C(211)–P(2)–Pt	112.8(4)
		C(211)–P(2)–C(2)	106.5(11)
		C(211)–P(2)–C(201)	107.9(6)

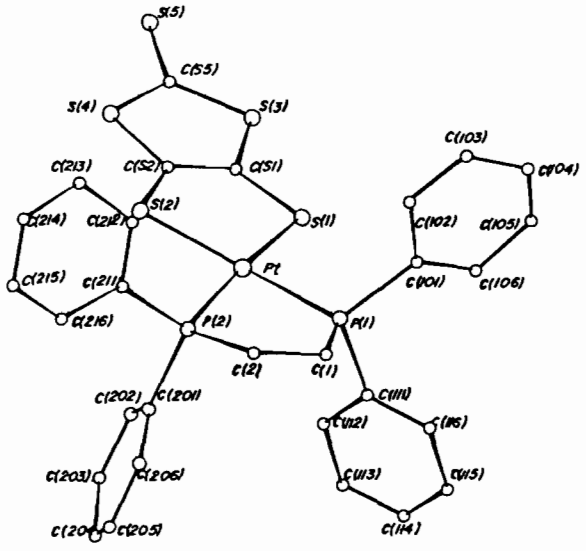

Fig. 1. Molecular structure of Pt(dmit)(dppe) and atom-labelling scheme.

2.311(3) Å, is identical to the value, 2.312(4) Å, observed in the $TTF[Pt(dmit)_2]_3$ compound [2] in which the Pt atom is coordinated to two dmit ligands. The S(1)...S(2) non bonding distance is similar to that observed in $[Ni(dmit)_2]^{n-}$ complexes [1, 20], but as the Pt–S bond length is larger than the Ni–S bond length, the S–Pt–S bond angle (90.0(1)°) is smaller than the S–Ni–S corresponding bond angle (mean value 92.3°). The environment of the Pt atom can be described as square-planar with a very slight tetrahedral distortion (deviations of atoms from their least-squares plane: Pt, 0.009(3); P(1), 0.088(3); P(2), −0.089(3); S(1), −0.090(3); S(2), 0.078(3). The Pt, S(1), S(2), C(S1), C(S2), S(3), and S(4) atoms are nearly in the sample plane (deviations of these atoms from their least-squares plane: −0.005(3), 0.006(3), 0.003(3), −0.001(11), −0.003(13), −0.004(3), 0.002(3) Å, respectively) and the C(5) and S(5) atoms deviate by 0.070(14) and 0.205 Å from this plane.

In previous studies on the $[Ni(dmit)_2]^{n-}$ series [1], it was discussed how very little information on the oxidation state, *i.e.* on the extent of electronic delocalization in the coordinated $dmit^{2-}$ ligand could be gained from structural observation. However, it is interesting to note that the $dmit^{2-}$ bond distances in Pt(dmit)(dppe) compare well with those observed for $TTF[Pt(dmit)_2]_3$ [2] and $(n\text{-}Bu_4N)[Ni(dmit)_2]$ [20], *i.e.* for complexes in which the formal oxidation state of the metal is higher than two.

In spite of the nearly planar configuration of the Pt(dmit) fragment, there is no close stacking of the Pt(dmit)(dppe) molecules in the crystal, due to steric hindrance caused by the bulky dppe ligand. In the stacked dmit metal complexes previously studied [1, 2] a large number of intermolecular S...S distances shorter than the sum of Van der Waals radii (3.70 Å) have been observed, and account for the unusual electrical behaviour of these compounds. In Pt(dmit)(dppe), only one such short intermolecular S...S contact is observed between the S(5) atoms of two independent molecules, related by a conversion centre (3.382(3) Å).

In conclusion, the determination of the crystal structure of Pt(dmit)(dppe) confirms the previously reported [4] characterization of this compound as a mononuclear complex and indirectly substantiates the hypothesis of the 'half-opening' mechanism that we have proposed for the formation of the derived metal-tetrathiolato polymers [5].

Redox Behaviour of the M(dmit)(dppe) and Pt(dmit)$(PPh_3)_2$ Complexes

The cyclic voltammetry parameters for the oxidation and reduction of the studied complexes are listed in Table IV. The Ni(dmit)(dppe) complex undergoes both a quasi-reversible one-electron reduction step and a reversible one-electron oxidation step (Fig. 2a). The reduction potential has a relatively high value ($E_{1/2}$ = −1335 mV) and is intermediate between the values observed for the maleonitriledithiolate-dppe complex Ni(mnt)(dppe) (−1200 mV) [21], the toluenedithiolate-dppe complex $Ni(CH_3C_6H_3S_2)$(dppe) (−1590 mV [21]), and the 1,2-diphenyl-1,2-ethenedithiolate-dppe complex $Ni(Ph_2C_2S_2)$-(dppe) (−1680 mV) [22]). The oxidation potential of Ni(dmit)(dppe) ($E_{1/2}$ = 556 mV) is slightly higher than that of the $Ni(Ph_2C_2S_2)$(dppe) complex (480 mV [22]).

The Pt(dmit)(dppe) complex undergoes at E_{pc} = −1710 mV an irreversible two-electron reduction step (Table IV and Fig. 2b). Both Pt(dmit)(dppe) and Pt(dmit)$(PPh_3)_2$ do not undergo reduction at least in the available potential range of the CH_2Cl_2 solvent (−2000 to +1500 mV). These results reflect the relative instability of the supposedly univalent Pd(I) and Pt(I) complexes compared with the corresponding Ni(I) complex (see below).

By contrast, and as in the case of the nickel complex analogue, the Pd(dmit)(dppe) and Pt(dmit)-(dppe) complexes undergo a reversible one-electron

TABLE IV. Cyclic Voltammetry Parameters for the Reduction and Oxidation of the M(dmit)(dppe) (M = Ni, Pd, Pt) and Pt-(dmit)$(PPh_3)_2$ Complexes[a]

Complex	Reduction						Oxidation					
	E_{pc}	E_{pa}	ΔE	$E_{1/2}$	n	I_{pc}/I_{pa}	E_{pa}	E_{pc}	ΔE	$E_{1/2}$	n	I_{pa}/I_{pc}
Ni(dmit)(dppe)	−1440	−1230	210	−1335	1	0.7	595	517	78	556	1	0.9
Pd(dmit)(dppe)	−1710				2		591	535	56	563	1	0.9
Pt(dmit)(dppe)							623	561	62	592	1	1
Pt(dmit)$(PPh_3)_2$							626	534	92	580	1	0.45

[a] 10^{-3} M in CH_2Cl_2 at *ca.* 290 K. Pt disc electrode (area 3.14 mm^2). Scan rate: 0.1 V s^{-1}. Supporting electrolyte: $(n\text{-}Bu_4N)ClO_4$ 0.1 M. Reference electrode: Ag/AgCl 0.1 M KCl. E_{pc}, E_{pa}, $E_{1/2}$ potential values are in mV. n: number of electrons exchanged. I_{pc}/I_{pa}: ratio of the peak intensities.

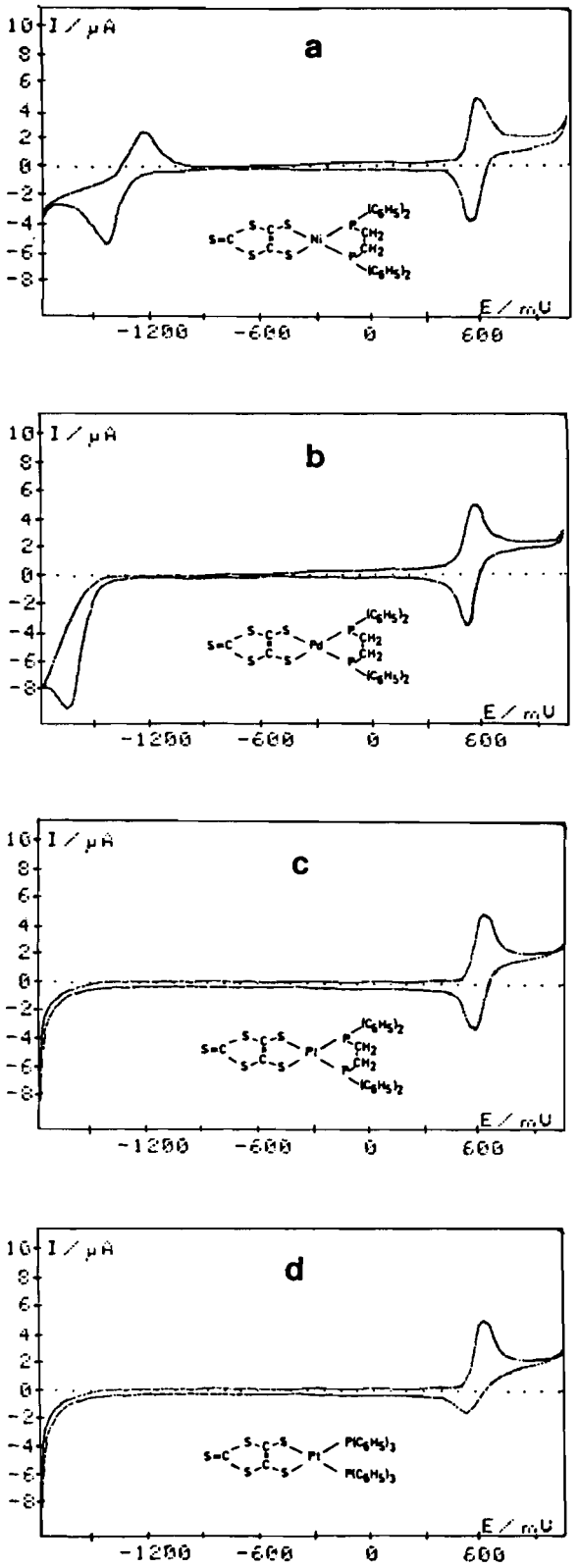

Fig. 2. Cyclic voltammogram of the redox process for (a) Ni(dmit)(dppe), (b) Pd(dmit)(dppe), (c) Pt(dmit)(dppe), and (d) Pt(dmit)$(PPh_3)_2$. CH_2Cl_2 solvent at *ca.* 290 K.

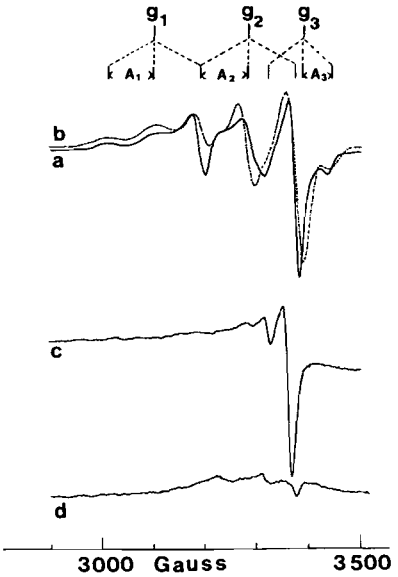

Fig. 3. EPR spectra of $[Ni(dmit)(dppe)]^-$ electrogenerated in CH_2Cl_2 at 210 K: (a) (——) frozen solution spectrum at 110 K; (b) (- - - -) simulated spectrum with: $g_1 = 1.995$, $g_2 = 2.055$, $g_3 = 2.170$; $A_1 = 154, A_2 = 254, A_3 = 274 \times 10^{-4}$ cm^{-1} for the $[Ni(dmit)(dppe)]^-$ majority species (92.7%), and with $g_\perp = 1.995$, $g_\parallel = 2.008$, band width = 50 MHz for an organic radical impurity (7.3%); (c) frozen solution spectrum at 110 K after warming the solution at 290 K for 10 s and freezing again; (d) frozen solution spectrum at 110 K after warming the solution at 290 K for 30 s and freezing again.

oxidation step at similar $E_{1/2}$ values (Table IV and Fig. 2b, c). The Pt(dmit)$(PPh_3)_2$ complex undergoes a quasi-reversible oxidation step (Fig. 2d). This oxidation step becomes irreversible in the presence of an excess of added PPh_3. This is opposite to what was observed for the reduction of Ni(mnt)$(PPh_3)_2$ [21].

EPR Spectrum of the Reduced Ni(dmit)(dppe) Complex

The EPR spectra of the product of the electrolysis of Ni(dmit)(dppe) at a potential below that of the reduction process shows anisotropy in the g values and hyperfine coupling to two equivalent ^{31}P nuclei Fig. 3a). However no satisfactory simulation of this experimental spectrum could be obtained by fitting the g_1, g_2, g_3 and A_1, A_2, A_3 parameters using the method and programs described in 'Experimental' [16, 17]. In particular, the high intensity of the experimental line at $g \sim 2.007$ could not be fitted. It could be suspected that this line was due to an organic radical impurity and this was confirmed by the following experiment: after warming the initial frozen solution at 290 K for 10 s and freezing again, the spectrum of the $[Ni(dmit)(dppe)]^-$ electrogenerated species nearly disappears and is replaced by a narrow single line at $g = 2.007$ typical of an organic

radical impurity (Fig. 3c). This impurity is not stable and finally vanishes as shown by the decrease of the intensity of this line when warming again the frozen solution at 290 K for 30 s and freezing again (Fig. 3d).

With this information at hand, the experimental spectrum could be fitted (Fig. 3b) by superposing to the spectrum of the $[Ni(dmit)(dppe)]^-$ majority species, a 'parasitic' spectrum corresponding to the organic radical impurity with $g_\perp = 1.995$ and $g_\parallel = 2.008$ and a line width of 16×10^{-4} cm^{-1}. The relative percentage of the $[Ni(dmit)(dppe)]^-$ species and of the organic impuritiy, 92.7 and 7.3%, respectively, can be obtained by using a refinement program based on the SIMPLEX methods [18]. The final simulation yields the following values for $[Ni(dmit)(dppe)]^-$: $g_1 = 2.170$, $g_2 = 2.055$, $g_3 = 1.995$, $A_1 = 274, A_2 = 254, A_3 = 154 \times 10^{-4}$ cm^{-1}.

The g values for the $[Ni(dmit)(dppe)]^-$ species are of comparable magnitude to those observed for related complexes involving the dppe ligand [21–24]. It has been shown that in these complexes ($[Ni(R_2NCS_2)(dppe)]^-$ [24], $[Ni(mnt)(dppe)]^-$ [21], $[Ni(Ph_2C_2S_2)(dppe)]^-$ [22], and [Ni(SacSac)-(dppe)] [23]), the unpaired electron is mainly localized on the Ni atom. The similarity in g values for these and the $[Ni(dmit)(dppe)]^-$ complex of the present study strongly suggests that this complex, too, should be regarded as a nickel(I) species.

EPR Spectra of the Oxidized M(dmit)(dppe) (M = Ni, Pd, Pt) and Pt(dmit)(PPh$_3$)$_2$ Complexes

The electrolysis of the M(dmit)(dppe) complexes (M = Ni, Pd, Pt) at a potential above that of the oxidation process, produced frozen solution spectra that showed no resolved ^{31}P hyperfine coupling (Figs. 4–6). The simulated spectrum for $[Ni(dmit)-(dppe)]^+$ was obtained with $g_x = g_y = 1.96$ and $g_z = 2.36$. The line width being *ca.* 160×10^{-4} cm^{-1}, the lines corresponding to the A_1, A_2 and A_3 coupling constants (estimated less than 50×10^{-4} cm^{-1}) cannot be seen on such spectra. The fact that the spectra of all three $[M(dmit)dppe]^+$ complexes are identical when going from nickel to palladium and platinum, the magnitude of the g_1 value (2.36 compared to ~2.00 generally observed for Ni(III) complexes [25]) and the absence of ^{31}P hyperfine coupling, strongly suggest that the unpaired electron is mainly delocalized on the dmit ligand and that these complexes should be regarded as M(II) species.

Whereas the spectra of the $[M(dmit)dppe]^+$ complexes are identical, the stability of these complexes is dependent on the nature of the metal. During the oxidation of the Ni(dmit)(dppe) complex, the initial yellow colour of the solution turns to purple. After warming the initial frozen solution at 290 K for 10 to 30 s and freezing again the intensity of the spectrum of $[Ni(dmit)(dppe)]^+$ decreases

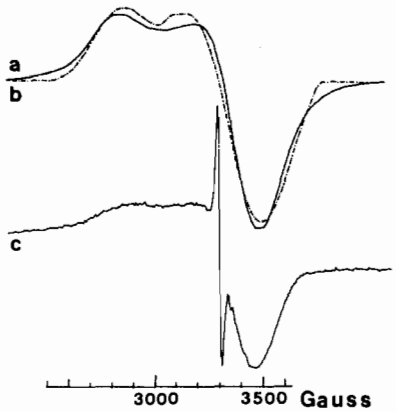

Fig. 4. EPR spectra of $[Ni(dmit)(dppe)]^+$ electrogenerated in CH_2Cl_2 at 210 K: (a) (——) frozen solution spectrum at 110 K; (b) (·····) simulated spectrum with $g_x = g_y = 1.96$, and $g_z = 2.36$, (c) frozen solution spectrum at 110 K after warming the solution at 290 K for 10 to 30 s.

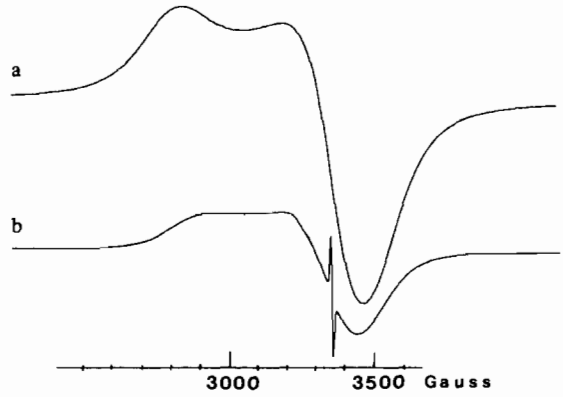

Fig. 5. EPR spectra of $[Pd(dmit)(dppe)]^+$ electrogenerated in CH_2Cl_2 at 210 K: (a) frozen solution spectrum at 110 K; (b) frozen solution spectrum at 110 K after warming the solution at 290 K for 30 s.

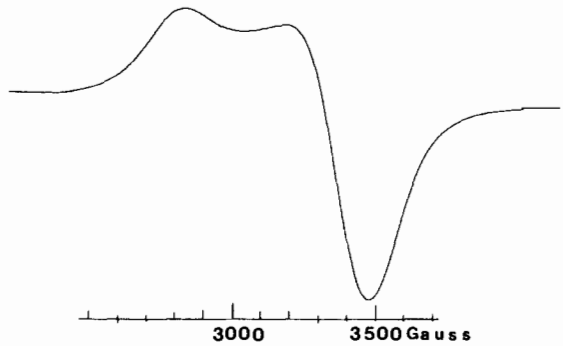

Fig. 6. EPR spectra of $[Pt(dmit)(dppe)]^+$ electrogenerated in CH_2Cl_2 at 210 K.

and a new narrow single line, characteristic of an organic radical species, is observed at $g \sim 2.04$ (Fig. 4). The intensity of this line firstly increases and the colour of the solution turns back to yellow when

the solution is warmed, but this signal eventually vanishes when the solution is kept at room temperature for a period of time longer than 1 min. During the oxidation of Pd(dmit)(dppe), the colour of the solution turns from orange to blue and a similar organic radical signal is observed at $g \sim 2.01$ (Fig. 5). However, this organic radical species is stable for a long period of time and coexists with the $[Pd(dmit)(dppe)]^+$ species. In the case of the Pt(dmit)(dppe) complex, the colour of the solution turns from yellow–orange to blue during the oxidation. However, when warming the frozen solution at 290 K for 30 s and freezing again, no organic radical line is observed (Fig. 6). The platinum compound appears to be the most stable complex of the $[M(dmit)(dppe)]^+$ series.

On the other hand, the $[Pt(dmit)(PPh_3)_2]^+$ oxidized species seems to be much less stable. The electrolysis of $Pt(dmit)(PPh_3)_2$ at a potential above that of the quasi-reversible oxidation process produced no frozen solution EPR spectra. It is interesting to note that during the oxidation the initial orange colour of the solution turns to blood-red and this colour persists even at room temperature for more than 24 h. The electrolysis of a solution of $Pt(dmit)(PPh_3)_2$ with excess PPh_3 present produced a very weak frozen solution EPR signal centered at $g \sim 2.12$ (line width $\sim 450 \times 10^{-4}$ cm^{-1}). This signal disappears after freeze–thawing experiments and a narrow line typical of an organic radical is observed at $g \sim 2.00$. In this case, the initial orange colour of the solution remains unchanged during the oxidation and the subsequent freeze–thawing cycles, and the organic radical species seems to be stable even at room temperature for several hours. These complex oxidation processes, probably followed by chemical reaction of the electrogenerated species, were not further investigated.

Conclusions

The electrochemical behaviour of the studied $M(dmit)(Phos)_2$ complexes and the stability of the derived electrogenerated species are dependent on the nature of the metal M. In the case of Ni(dmit)(dppe), the reduction is metal-based and $[Ni(dmit)(dppe)]^-$ is a nickel(I) species; however this species is unstable at room temperature and an organic radical is formed. The corresponding $[Pd(dmit)(dppe)]^-$ and $[Pt(dmit)(dppe)]^-$ complexes and the $[Pt(dmit)(PPh_3)_2]^-$ complex cannot be obtained because of their low stability.

By contrast, the oxidation of the M(dmit)(dppe) complexes (M = Ni, Pd, Pt) is ligand-based and the unpaired electron of the $[M(dmit)(dppe)]^+$ oxidized species is mainly localized on the dmit ligand. Similar results have been previously obtained for parent $M(Ph_2C_2S_2)(dppe)$ complexes [22]. In the $[M(dmit)dppe]^+$ series the stability of the oxidized species increases when going from nickel to palladium and to platinum. The oxidation of $Pt(dmit)(PPh_3)_2$ is quasi-reversible and no $[Pt(dmit)(PPh_3)_2]^+$ species could be detected by EPR spectroscopy. In the presence of an excess of the PPh_3 ligand, the oxidation of $Pt(dmit)(PPh_3)_2$ becomes irreversible.

If the studied M(dmit)(dppe) complexes may be considered as molecular model compounds for the metal-tetrathiolato polymers, it can be inferred from the previous results that the partial oxidation of the $(MC_2S_4^{2-})_n$ polymers which leads to the conductive $(MC_2S_4^{x-})_n$ polymers [5], is also ligand-based and that these polymers are M(II) compounds. Hence, the degree of partial oxidation results from the accessibility of a number of partial oxidation states for the C_2S_4 ligand. This hypothesis is supported by several other observations: Conductive metal-tetrathiooxalato polymers have been recently described by Reynolds *et al.* [26]; the preliminary results of compared EXAFS and LAXS (Large Angle X-ray Scattering) structural studies of both the nickel-tetrathiolato $(NiC_2S_4^{x-})_n$ polymer and the nickel-tetrathiooxalato $(NiC_2S_4)_n$ polymer show that in both polymers the bond lengths and angles are very comparable [27]. Moreover, it has been shown that air oxidation of the copper complex of the oxygen-analog ligand of dmit, $(AsPh_4)_2[Cu(dmdto)_2]$ (H_2dmdto = 4,5-dimercapto-1,3-dithia-2-one), yields a dinuclear complex, $(AsPh_4)_2[(dmdto)Cu(\mu\text{-}C_2S_4)\text{-}Cu(dmdto)]$, in which the central (C_2S_4) unit has been proved by X-ray diffraction studies to be the dithiooxalato ligand [28]. Both results confirm the possible conversion by oxidation of the tetrathiolate ligand into the tetrathiooxalate ligand, and hence, the accessibility of different oxidation states of the C_2S_4 ligand. Finally, the partially oxidized nickel-tetrathiolato polymer, $[Na_{0.31}(NiC_2S_4)]_n$, exhibits a low magnetic moment at room temperature and a narrow EPR signal, which are probably due to delocalized spins along the polymer chain rather than to Ni(III) centres [5].

Acknowledgements

Financial assistance through the 'Actions Intégrées Franco-Espagnoles' Programme, from C.A.I.C.Y.T. (n. 0855/84) and the Generalitat de Catalunya (CIRIT), is gratefully acknowledged.

References

1 L. Valade, P. P. Legros, M. Bousseau, P. Cassoux, M. Garbauskas and L. V. Interrante, *J. Chem. Soc., Dalton Trans.*, 783 (1985).
2 M. Bousseau, L. Valade, J.P. Legros, P. Cassoux, M.

Garbauskas and L. V. Interrante, *J. Am. Chem. Soc., 108*, 1908 (1986).
3 L. Brossard, M. Ribault, M. Bousseau, L. Valade and P. Cassoux, *C.R. Acad. Sci. Paris, Sér. II, 302*, 205 (1986); L. Brossard, M. Ribault, L. Valade and P. Cassoux, *Physica B, 143*, 378 (1986).
4 R. Vicente, J. Ribas and P. Cassoux, *Nouv. J. Chim., 8*, 653 (1984).
5 R. Vicente, J. Ribas, P. Cassoux and L. Valade, *Synth. Met., 13*, 265 (1986).
6 *US Pat. no. 4111857* (1978) to E. M. Engler, K. H. Nichols, V. V. Patel, N. M. Rivera and R. R. Schumaker; N. M. Rivera and E. M. Engler, *J. Chem. Soc., Chem. Commun.*, 184 (1979).
7 H. Poleschner, W. John, G. Kempe, E. Hoyer and H. Fanghänel, *Z. Chem., 18*, 345 (1978).
8 G. E. Holdcroft and A. E. Underhill, *Synth. Met., 10*, 427 (1985).
9 H. Poleschner, E. Fanghänel, W. John, F. Hoppe and S. Roth, *J. Prakt. Chem., 325*, 957 (1983).
10 P. Main, S. E. Fiske, S. L. Hull, L. Lessinger, G. Germain, J.-P. Declercq and M. M. Woolfson, 'MULTAN', an automatic computer program for crystal structure determination from X-ray diffraction data, University of York, U.K. and University of Louvain, Belgium, 1980.
11 G. M. Sheldrick, 'SHELX-76', program for crystal structure determinations, University of Cambridge, 1976.
12 'International Tables for X-Ray Crystallography', Vol. IV, Kynoch Press, Birmingham, U.K. 1974.
13 P. Cassoux, R. Dartiguepeyron, P. L. Fabre and D. de Montauzon, *L'Actualité Chimique*, 79 (1985); *Electrochim. Acta, 11*, 1485 (1985).
14 M. M. Baizer, 'Organic Electrochemistry', Dekker, New York, 1973, p. 219.
15 C. Cross, J.-P. Costes and D. de Montauzon, *Polyhedron, 3*, 585 (1984).
16 M. J. Nilges, *Ph.D. Thesis*, University of Illinois, Urbana, 1979; R. L. Bedford and M. J. Nilges, 'Computer simulation of powder spectra', *EPR Symposium, St Rocky Mountain Conference*, Denver, 1979; A. M. Maurice, *Ph.D. Thesis*, University of Illinois, Urbana, 1980.
17 J. A. Weil, *J. Magn. Res., 18*, 113 (1975).
18 F. James and M. Roos, 'MINUIT program', a system for function minimization and analysis of the parameters errors and correlations, *Comput. Phys. Commun., 10*, 345 (1975).
19 G. G. Messmer, E. L. Amma and J. A. Ibers, *Inorg. Chem., 6*, 725 (1967).
20 O. Lindqvist, L. Sjölin, J. Sieler, G. Steimecke and E. Hoyer, *Acta Chem. Scand., Ser. A, 33*, 445 (1979); O. Lindqvist, L. Andersen, J. Sieler, G. Steimecke and E. Hoyer, *Acta Chem. Scand., Ser. A, 36*, 855 (1982).
21 G. A. Bowmaker, P. D. W. Boyd and G. K. Campbell, *Inorg. Chem., 21*, 2403 (1982).
22 G. A. Bowmaker, P. D. W. Boyd and G. K. Campbell, *Inorg. Chem., 22*, 1208 (1983).
23 G. A. Bowmaker, P. D. W. Boyd, M. Zvagulis, K. J. Cavell and A. F. Masters, *Inorg. Chem., 24*, 401 (1985).
24 G. A. Bowmaker, P. D. W. Boyd, G. K. Campbell, J. M. Hope and R. L. Martin, *Inorg. Chem., 21*, 1152 (1982).
25 R. I. Haines and A. McAuley, *Coord. Chem. Rev., 39*, 77 (1981).
26 J. R. Reynolds, F. E. Karasz, C. P. Lillya and J. C. W. Chien, *J. Chem. Soc., Chem. Commun.*, 268 (1985).
27 C. Faulmann, P. Cassoux, J. R. Reynolds and C. A. Jolly, unpuplished results.
28 R. Vicente, J. Ribas, S. Alvarez, A. Segui, X. Solans and M. Verdaguer, *Inorg. Chem.*, in press.